INTRICATE STUDY OF HYDROTHERMALLY-SYNTHESIZED HEXAGONAL $K_2W_4O_{13}$ NANOWIRES FOR THE ADSORPTION AND PHOTODEGRADATION OF ORGANIC DYES AND HEAVY METAL IONS

Lim Dillion (4S3), Bryan Lee Chong Han (4P1), Ho Shanley (4P1)

Group 1-23

Abstract

Water pollution is a pertinent issue today, with pollutants such as dyes and metal ions causing health issues. Potassium tungstate ($K_2W_4O_{13}$) nanowires show huge potential in mitigating water pollution. However, the conventional synthesis method involves calcination, which is energy-intensive and economically unfriendly. In the present study, $K_2W_4O_{13}$ nanowires were synthesized through a more eco-friendly hydrothermal method which does not require calcination. The $K_2W_4O_{13}$ nanowires synthesized were evaluated in terms of their adsorption capabilities on brilliant green dye and lead(II) ions. Mechanism of adsorption was studied using isotherms. Results showed that $K_2W_4O_{13}$ nanowires synthesized are cylindrical in shape. $K_2W_4O_{13}$ nanowires are also comparable to commercial activated carbon in the removal of brilliant green dye and lead(II) ions respectively, removing 99.9% of brilliant green dye and 99.3% lead(II) ions. Interestingly, besides being an adsorbent, $K_2W_4O_{13}$ nanowires could double up as a photocatalyst which can degrade dyes in the presence of visible light They are also comparable to titanium dioxide in photodegrading methyl orange dye, removing 99.9% of the dye. The $K_2W_4O_{13}$ nanowires synthesized have great potential to be used in wastewater treatment to remove dyes and metal ions.

1. Introduction

The rapid growth of industries has led to water pollution becoming a pertinent issue in today's society. Pollution is associated with an estimated 9 million deaths a year, with water pollution contributing 1.8 million deaths (Mayor, 2017).

One common pollutant which is commonly discharged into water bodies is dye. In the textile industry, up to 200,000 tonnes of these dyes are lost to effluents every year due to the inefficiency of the dyeing process (Ogugbue & Sawidis, 2011), presenting major environmental problems for developing countries like Bangladesh (Yardley, 2013). One example of dye is brilliant green, a toxic cationic dye that is widely used in the textile and printing industries (Nandi, Goswami & Purkait, 2008). Discharge of brilliant green into the hydrosphere has an adverse effect on humans, causing irritation to the gastrointestinal and respiratory tract, as well as symptoms such as nausea, vomiting and diarrhoea (Gogate &

Bhosale, 2013). Another example of dye is methyl orange, an anionic dye which is extensively used in the textile industry and has harmful effects on human health (Valica & Hostin, 2016). Furthermore, it is highly soluble in water and persistent in polluted water, having a long degradation time, further exacerbating the problem it causes (Azami, Bahram, Nouri & Naseri, 2012).

Another type of pollutant commonly found in water is heavy metal ions, such as lead(II) ions, which may cause many serious disorders like anemia, kidney diseases, nervous disorders and even deaths (Naseem, 2012). Infants and young children are especially sensitive to even low levels of lead, which may contribute to behavioural problems, learning deficits and lowered IQ (Wani, Ara, Usmani, 2015).

Current methods of removing dyes include chemical coagulation, adsorption (Gecgel, Ozcan & Gurpinar, 2013) and advanced oxidation processes (Silva et al., 2013). On the other hand, current treatment methods for removal of lead(II) ions from industrial wastewater include chemical precipitation, ion exchange, membrane separation, and adsorption (Dakhil, 2015). Among these techniques, adsorption is a promising method to treat waste water containing both dyes and lead(II) ions, due to the high efficiency, low cost and ease of carrying out (Keiteb, Saion, Zakaria & Soltani, 2016). Although activated carbon is the most popular adsorbent used, its generation is difficult and costly, which restricts its application in developing countries (Kyriakopoulos & Doulia, 2006).

Tungsten-based compounds have gained interest in recent years, with applications including solar filters (Li *et al.*, 2016), CT imaging of tumors (Zhou, Kong & Yu, 2014), and gas sensors (Supothina, Suwan & Wisitsoraat, 2014). Potassium tungsten oxides (K_xWO_3, $0<x<1$) are one type of non-stoichiometric tungsten compounds that are formed when potassium atoms partially occupy tunnels in the WO_3 framework formed by axial oxygen sharing of WO_6 octahedra (Appendix, Pg 16). $K_2W_4O_{13}$ in particular, displayed good water purification properties and exhibited acid and alkali resistance and good reusability properties (Huang, Wei, Sun, Mao & Ni, 2019).

However, $K_2W_4O_{13}$ nanowires displayed poor adsorption capabilities on anionic compounds (Zhao, Ping, Di & Zheng, 2015). Further research revealed that tungsten-based compounds have good photocatalytic properties (Khan et al., 2019), hence photocatalytic degradation is a promising avenue to explore for the removal of anionic dyes such as methyl orange.

Based on several studies (Wu *et al.*, 2017; Liu *et al.*, 2013), the conventional way of synthesising $K_2W_4O_{13}$ nanowires involves calcination, which is highly energy-intensive and hence limits its use as an adsorbent.

2. Objectives and Hypotheses

The objectives of this study are to synthesise $K_2W_4O_{13}$ nanowires through a less energy intensive hydrothermal method with sodium tungstate dihydrate and potassium sulfate as precursors, to investigate the effectiveness of synthesised $K_2W_4O_{13}$ nanowires in adsorbing lead(II) ions and brilliant green dye (a cationic dye) and in photodegrading methyl orange dye (an anionic dye).

The hypotheses of the study are that $K_2W_4O_{13}$ nanowires can be successfully synthesised through a hydrothermal method and the synthesised $K_2W_4O_{13}$ nanowires are effective in adsorbing lead(II) ions and brilliant green dye as well as in photodegrading methyl orange dye.

3. Materials and Methods

3.1 Materials

Potassium sulfate (K_2SO_4), hydrogen peroxide (H_2O_2) and lead(II) nitrate ($Pb(NO_3)_2$) were procured from GCE Laboratory Chemicals. Sodium tungstate dihydrate ($NaWO_4{\cdot}2H_2O$), titanium (IV) dioxide (TiO_2), Methyl Orange ($C_{14}H_{14}N_3NaO_3S$) and Brilliant Green ($C_{27}H_{34}N_2O_4S$) were purchased from Sigma-Aldrich. Hydrochloric acid (HCl) was procured from Scharlau.

3.2 Synthesis of $K_2W_4O_{13}$ nanowires

1.98g of sodium tungstate dihydrate and 5.00g of potassium sulfate were dissolved in 35ml of deionised water. The pH of the mixture was adjusted to 1.10-1.20 using 6M hydrochloric acid. The mixture was refluxed at 100°C for 4 hours. The precipitate formed was centrifuged and washed with deionised water until pH was neutral. The final product was vacuum dried at 60°C until constant mass and ground into fine powder using a mortar and pestle. The reactions which lead to the formation of $K_2W_4O_{13}$ nanowires are proposed to be (Equation 1-3):

$$Na_2WO_4\,(aq) + 2HCl\,(aq) \rightarrow H_2WO_4\,(s) + 2NaCl\,(aq) \quad (1)$$

$$3H_2WO_4\,(s) \rightarrow 3WO_3{\cdot}0.33H_2O(s) + 2H_2O\,(l) \quad (2)$$

$$12WO_3{\cdot}0.33H_2O(s) + 3K_2SO_4\,(aq) \rightarrow 3K_2W_4O_{13}\,(s) + 3H_2SO_4\,(aq) + H_2O\,(l) \quad (3)$$

The $K_2W_4O_{13}$ nanowires synthesized were characterised with Scanning Electron Microscopy (SEM), Energy Dispersive Spectroscopy (EDS) and X-Ray Diffraction (XRD).

3.3 Batch adsorption studies

3.3.1 Effect of initial concentration

The adsorbate solutions were prepared by dissolving different amount of AR grade brilliant green dye and $Pb(NO_3)_2$ in deionized water respectively to achieve solutions of concentration ranging from 50 mg/L to 800 mg/L of brilliant green dye and lead(II) ion. Batch adsorption studies were carried out with beakers containing 20 ml of brilliant green dye solution or lead(II) ion solution of different concentrations and 0.10 g of $K_2W_4O_{13}$ nanowires. The mixtures were stirred for 24 hours, after which they were centrifuged and the supernatant analysed for residual brilliant green dye and lead(II) ion using a UV-Vis Spectrophotometer (Shimadzu UV1800) at 625 nm and an Atomic Absorption Spectrophotometer (Shimadzu 6300) respectively. The set-ups also included a control without any $K_2W_4O_{13}$ nanowires. Five replicates were conducted for each concentration.

The equilibrium concentration data were fitted into Langmuir and Freundlich isotherms (Appendix, Pg 14-16) to determine the adsorption mechanisms and maximum adsorption capacity.

Adsorption of phosphate and lead(II) ion was evaluated in terms of adsorption capacity (Q) and removal efficiency (R). The adsorption capacity (Q) was calculated in mg/g according to the following formula:

$$Q = \frac{(C_i - C_f)V}{M}$$

C_i = initial concentration; C_f = final concentration
V = volume of solution; M = mass of $K_2W_4O_{13}$ nanowires

Removal efficiency (R) was calculated in % according to the following formula:

$$R = \frac{(C_i - C_f)}{C_i} x100\%$$

C_i = initial concentration; C_f = final concentration

3.3.2 Determination of band gap of $K_2W_4O_{13}$ nanowires

The band gap of $K_2W_4O_{13}$ nanowires was calculated by determining its absorption edge wavelength from its UV-Vis spectrum before substituting it into the Planck-Einstein relation (Equation 4):

$$E_g = \frac{hc}{\lambda_{a.e.\ (nm)}} \qquad (4)$$

where E_g is the band gap, h is Planck's constant (6.6261×10^{-34} m^2 kg s^{-1}), c is the speed of light (2.9979×10^8 m s^{-1}) and $\lambda_{a.e.\ (nm)}$ is the wavelength of the absorption edge (in nm).

The absorption edge was determined by finding the tangent of the maximum point of the derivative of its UV-Vis spectrum and determining the point at which it cuts the x-axis.

3.3.3 Photodegradation studies and effect of volume of H_2O_2

Photodegradation studies on the effect of volume of H_2O_2 were carried out with beakers containing 20ml of 50 mg/L methyl orange dye solution, 0.10g of $K_2W_4O_{13}$ nanowires and varying amounts of H_2O_2 from 0 - 2 ml. The mixtures were stirred for 24 hours in darkness or under the irradiation of visible light by a 14W fluorescent tube, after which they were centrifuged and the supernatant analysed for residual methyl orange dye using a UV-Vis Spectrophotometer (Shimadzu UV1800) at 464 nm. The set-ups also included a control without any $K_2W_4O_{13}$ nanowires. Five replicates were conducted for each concentration. Removal efficiency as described in section 3.3.2 was determined. The effectiveness of $K_2W_4O_{13}$ nanowires in photodegrading methyl orange was compared with titanium dioxide, a conventional photocatalyst.

3.3.4 Comparing the performance of $K_2W_4O_{13}$ nanowires with commercial activated carbon and titanium dioxide

The effectiveness of $K_2W_4O_{13}$ nanowires was compared with commercial activated carbon, a conventional adsorbent used to remove brilliant green dye and lead(II) ions, as well as titanium dioxide, a conventional photocatalyst used to degrade methyl orange dye.

4. Result and Discussions

4.1 Characterisation of $K_2W_4O_{13}$ nanowires

4.1.1 SEM images of $K_2W_4O_{13}$ nanowires

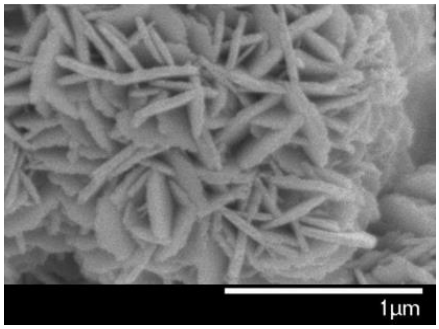

Figure 1: SEM image of $K_2W_4O_{13}$ nanowires

$K_2W_4O_{13}$ nanowires synthesized had aspect ratios (ratio of width to height) of 3.0 – 7.33 and were observed to be cylindrical in shape (Figure 1). Using ImageJ (a Java-based processing software), $K_2W_4O_{13}$ nanowires were determined to have an average length of 7.90 nm and an average diameter of 1.20nm. Sulfate ions are known to stimulate crystal growth along the *c*-axis, promoting the growth of 1D nanowires (Gu, Ma, Yang, Zhang & Yao, 2005) and the SEM image obtained concurs with this theory.

4.1.2 Energy-dispersive spectroscopy (EDS)

The presence of potassium, tungsten and oxygen (Figure 2) confirms the identity of the $K_2W_4O_{13}$ nanowires.

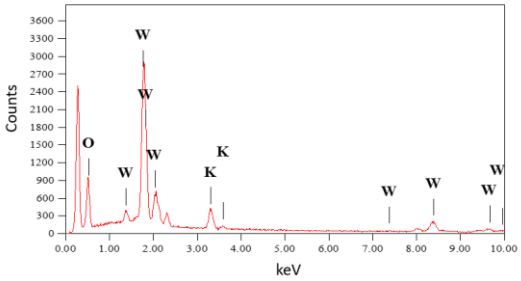

Figure 2: EDS of $K_2W_4O_{13}$ nanowires synthesized

4.1.3 X-Ray Diffraction (XRD)

The 2-theta peaks at 24.6° and 47.3° (Figure 3) are characteristic of $K_2W_4O_{13}$ nanowires while the 2-theta peaks at 12.2°, 21.4°, 28.4°, 30.9°, 37.3° and 47.3° are characteristic of orthorhombic tungsten oxide hydrate ($WO_3 \cdot 0.33H_2O$). The XRD pattern of $K_2W_4O_{13}$ nanowires synthesized is similar to those reported in literature (Huang, Wei, Sun, Mao & Ni, 2019).

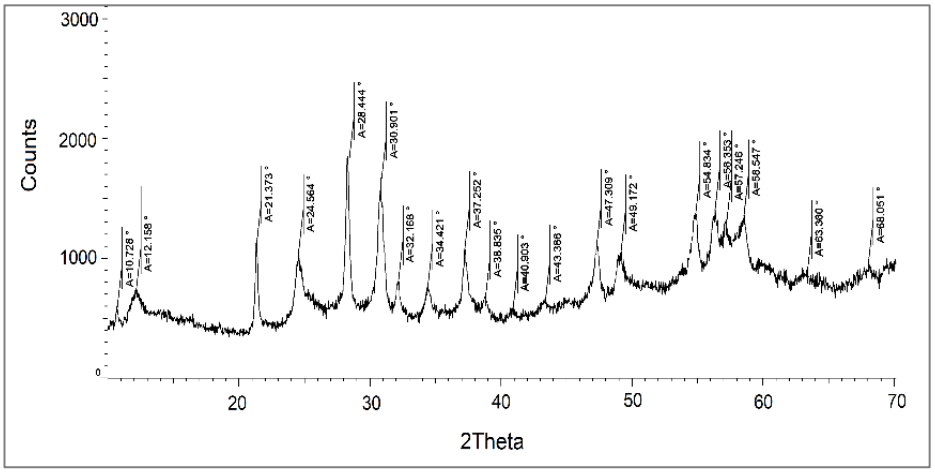

Figure 3: XRD pattern of $K_2W_4O_{13}$ nanowires synthesized

4.2 Batch Adsorption studies

4.2.1 Comparison of adsorption of brilliant green with $K_2W_4O_{13}$ nanowires and activated Carbon

$K_2W_4O_{13}$ nanowires are more effective than activated carbon in adsorbing brilliant green dye, adsorbing close to 100% of it (Figure 4). The difference in the percentage removal by $K_2W_4O_{13}$ nanowires and activated carbon is significant as the p-value of Mann-Whitney test is 0.00451 (<0.05).

Brilliant green dye is adsorbed via electrostatic attraction with the surface hydroxyl groups present due to weakly-bonded water molecules and W=O, leading to a negatively charged $K_2W_4O_{13}$ nanowires, promoting electrostatic attraction between the negatively charged $K_2W_4O_{13}$ nanowires with the cationic brilliant green (Huang, Wei, Sun, Mao & Ni, 2019). On the other hand, activated carbon removes brilliant green via π-π interactions between the π electrons in the aromatic rings of brilliant green dye and the aromatic rings of carbon present in activated carbon.

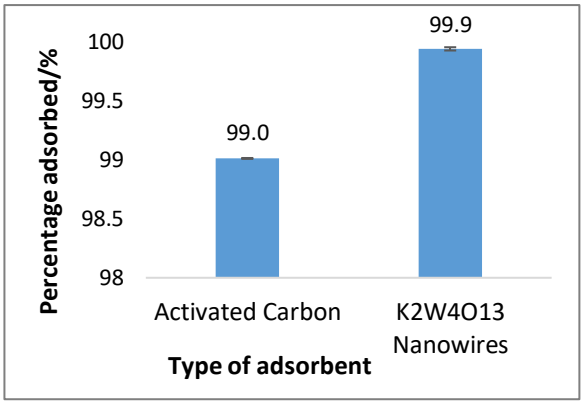

Figure 4: Adsorption of brilliant green dye by $K_2W_4O_{13}$ nanowires as compared to activated carbon

4.2.2 Comparison of adsorption of Pb^{2+} with $K_2W_4O_{13}$ nanowires and activated carbon

$K_2W_4O_{13}$ nanowires removes close to 100% of lead(II) ions (Figure 5), outperforming activated carbon. There is a significant difference in the percentage removal of lead(II) ions by $K_2W_4O_{13}$ nanowires and commercial activated carbon as the p-value of Mann-Whitney test is 0.00815 (< 0.05). The high percentage of adsorption of lead(II) ions by $K_2W_4O_{13}$ nanowires can be attributed to the ability of the H^+ ions from the W-OH groups and K^+ ions from $K_2W_4O_{13}$ to undergo ion-exchange with the Pb^{2+} ions. Furthermore, metal-ligand complexation between Pb^{2+} and $K_2W_4O_{13}$ increased its effectiveness as complexation minimised the system energy since energy was released upon complexation with the equatorial and axial oxygen atoms (Huang et al., 2020), hence removing them from the solution.

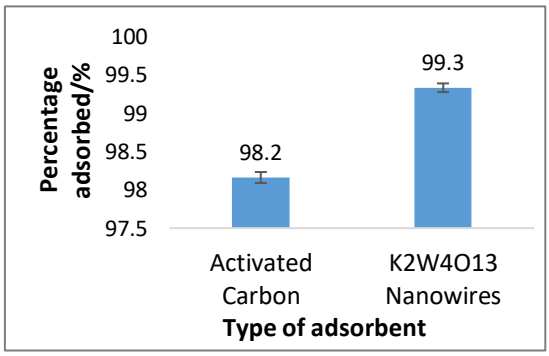

Figure 5: Adsorption of lead(II) ions by $K_2W_4O_{13}$ nanowires as compared to activated carbon

Activated carbon contains functional groups such as hydroxyl, phenol, ether and lactone groups which render it effective in binding to metal ions via dative bonds (Chen & Wu, 2004).

4.3 Isotherm Studies

The equilibrium concentration data of both brilliant green dye and lead(II) ions fit Langmuir isotherms (Appendix, Pg 14-16), suggesting that the adsorption is monolayer on a homogeneous surface. Maximum adsorption capacities on brilliant green dye and lead(II) ions were derived and compared with other adsorbents (Tables 1 and 2). The maximum adsorption capacity (Q_{max}) of $K_2W_4O_{13}$ nanowires on brilliant green dye is higher than that on lead(II) ions. Compared to several other adsorbents reported in literature, the Q_{max} of $K_2W_4O_{13}$ nanowires on both pollutants are higher, suggesting that it is an adsorbent with great potential to be used in wastewater treatment.

Table 1: Comparison of maximum adsorption capacity (Q_{max}) of different adsorbents on brilliant green dye

Adsorbent	(Q_{max}) (mg/g)	Reference
$K_2W_4O_{13}$ nanowires	476	This study
Mesoporous Ni-SBA-16	323	Shah, Din, Kanwal & Mirza, 2014
ZnO nanoparticles	238	Kataria & Garg, 2017
Activated carbon from pine fruit shell	219	Calvate, Lima, Cardoso & Das, 2010

Table 2: Comparison of maximum adsorption capacity (Q_{max}) of different adsorbents on lead(II) ions

Adsorbent	(Q_{max}) (mg/g)	Reference
$K_2W_4O_{13}$ nanowires	175	This study
Glutamic acid modified thermal activated sepiolite	128	Karaoğlu, Kula & Uğurlu, 2012
Mangoxide mineral	98	Sönmezaym, Öncel & Bektaş, 2012
Activated carbon coconut shell	27	Oganlalu et al., 2017

4.4 Determination of Band Gap of $K_2W_4O_{13}$ nanowires

The band gap of semiconductors is important in determining its photocatalytic activity of semiconductors. The calculation of band gap can be carried out using the Planck-Einstein relation (Figure 6). Conventional photocatalyst such as TiO_2 has a band gap higher than 3.2 eV and is unable to harness visible light efficiently for photodegradation as the photon energy of visible light ranges from 1.6 to 3.2 eV. In contrast, $K_2W_4O_{13}$ nanowires which have a lower band gap of 3.17 eV (Figure 6) is able to absorb visible light to degrade dye.

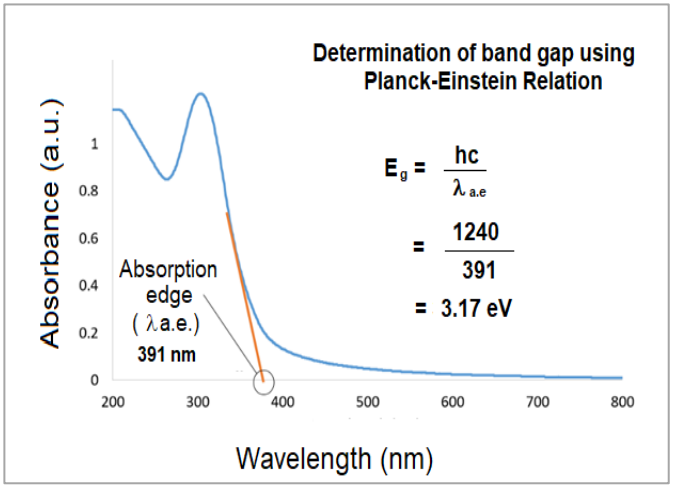

Figure 6: UV-Vis spectrum of $K_2W_4O_{13}$ nanowires for use in calculation of band gap

4.5 Photodegradation Studies

4.5.1 Effect of presence of visible light on degradation of methyl orange

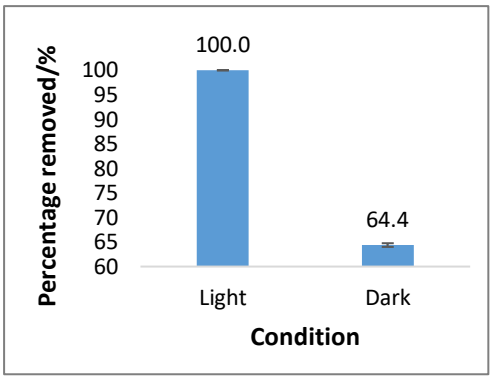

Figure 7: Comparison of removal of methyl orange in presence of visible light and darkness using 1ml H_2O_2

To determine the photocatalytic activity of $K_2W_4O_{13}$ nanowires, dye degradation experiments were conducted in darkness and under irradiation of visible light. Figure 7 compares the percentage of dye removed by $K_2W_4O_{13}$ nanowires in dark and light conditions. There is a significant difference in the percentage removal of methyl orange dye by $K_2W_4O_{13}$ nanowires with and without light as the p-value of Mann-Whitney test is 0.00604 (< 0.05). Amount of dye removed in the presence of visible light is significantly greater than that without light, suggesting that $K_2W_4O_{13}$ nanowires are indeed photocatalysts.

Methyl orange dye had a high photodegradation efficiency as the diazenyl group (-N=N-) of methyl orange was first protonated by a H^+ ion to form a -NH^+=N- group in methyl orange. H_2O_2 undergoes homolytic cleavage to form hydroxyl radicals (Equation 5). The hydroxyl radicals undergo a substitution reaction with the region of high electron density (=NH^+ and =N) and the intermediates then undergo further substitution reactions with the SO_3^- group and the amine group, eventually degrading the methyl orange molecule (Wang, Zhang, Chen, Zhang & Zhang, 2011).

$$H_2O_2 \xrightarrow{hv} 2HO\cdot \quad (5)$$

4.5.2 Comparison of degradation of methyl orange with $K_2W_4O_{13}$ nanowires and titanium dioxide

$K_2W_4O_{13}$ nanowires removes close to 100% of methyl orange dye (Figure 8). The percentage removal of methyl orange dye by $K_2W_4O_{13}$ nanowires is significantly greater than titanium dioxide as the p-value of Mann-Whitney test is 0.00397 (< 0.05). This is because titanium dioxide has a higher band gap of 3.20 eV (Yu, Hou, Li, Sun & Lee, 2013) and is not able to harness visible light effectively.

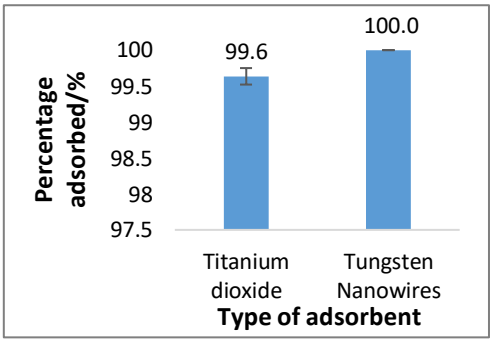

Figure 8: Adsorption of methyl orange by $K_2W_4O_{13}$ nanowires as compared to titanium dioxide

4.5.3 Effect of volume of H_2O_2 on photodegradation of methyl orange

$K_2W_4O_{13}$ nanowires photodegraded more than 99% of methyl orange dye when a minimum of 1ml of H_2O_2 was added (Figure 9). With an increase in the amount of H_2O_2 added, the degradation efficiency of methyl orange remains approximately constant, possibly due to a decrease in the concentration of $HO\cdot$ as excess H_2O_2 reacts with $HO\cdot$ to form hydroperoxyl radicals ($HO_2\cdot$) (Equation 6) (Barbusiński, 2009).

$$HO\cdot + H_2O_2 \rightarrow HO_2\cdot + H_2O \qquad (6)$$

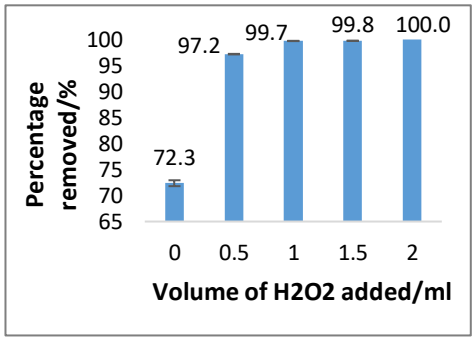

Figure 9: Photodegradation of methyl orange dye with varying amounts of H_2O_2

5. Conclusion and Future Work

$K_2W_4O_{13}$ nanowires have been successfully synthesized using $NaWO_4{\cdot}2H_2O$ and potassium sulfate via a simple hydrothermal method. Compared to the conventional method, the method employed in this study is less energy intensive as no calcination is required. The $K_2W_4O_{13}$ nanowires synthesized are more effective than activated carbon in adsorbing both brilliant green dye and lead(II) ions. The equilibrium experimental data is a good fit for Langmuir isotherm, suggesting that the adsorption of both brilliant green dye and lead(II) ions by $K_2W_4O_{13}$ nanowires is monolayer. The maximum adsorption capacities of $K_2W_4O_{13}$ nanowires for brilliant green dye and lead(II) ions were determined to be 476 mg g^{-1} and 175 mg g^{-1} respectively, which are higher than several adsorbents reported by other studies. Another interesting feature of $K_2W_4O_{13}$ nanowires is its photocatalytic activity. It was comparable to titanium dioxide in degrading methyl orange dye, with an optimum volume of 1ml of H_2O_2 being used in the presence of visible light. As $K_2W_4O_{13}$ nanowires are versatile and possess both adsorptive and photocatalytic properties, it has great potential to be used in water treatment plants to remove dyes and metal ions.

Possible extensions to this study include investigating the kinetics of adsorption of brilliant green dye and lead(II) ions by $K_2W_4O_{13}$ nanowires. The photodegradation mechanism of methyl orange could be confirmed by mass spectroscopy. Furthermore, in real life, wastewater contains multiple pollutants and hence it would be relevant to study whether the presence of other pollutants would affect the adsorption of brilliant green dye and lead(II) ions by $K_2W_4O_{13}$ nanowires. Finally the reusability of $K_2W_4O_{13}$ nanowires for multiple cycles of adsorption can be explored.

References

Azami, M., Bahram, M., Nouri, S., & Naseri, A. (2012). A central composite design for the optimization of the removal of the azo dye, methyl orange, from waste water using Fenton reaction. *Journal of the Serbian Chemical Society*. 77(2), 235-246.

Barbusiński, K. (2009). Fenton reaction - Controversy concerning the chemistry. *Ecological Chemistry And Engineering S, 16*(3), 347-358.

Calvete, T., Lima, E., Cardoso, N., Dias, S. & Ribeiro, E. (2010). Removal of Brilliant Green Dye from Aqueous Solutions Using Home Made Activated Carbons. *CLEAN - Soil Air Water*, *38*(5), 521-531.

Chen, P., & Wu, S. (2004). Acid/base-treated activated carbons: Characterisation of functional groups and metal adsorptive properties. Langmuir, *20*(6), 2233-42. DOI: 10.1021/la0348463

Dakhil, I.B (2005). Adsorption of lead from industrial effluents using rice husk. International *Journal of Engineering and Management Research*, *5*(1), 109-116.

Gecgel, U., Ozcan, G & Gurpinar, G.C. (2013). Removal of Methylene Blue from Aqueous Solution by Activated Carbon Prepared from Pea Shells (Pisum sativum). *Journal of Chemistry*, *2013*, 614083. Retrieved from https://www.hindawi.com/journals/jchem/2013/614083/.

Gogate, P.R., & Bhosale, G.S. (2013). Comparison of effectiveness of acoustic and hydrodynamic cavitation in combined treatment schemes for degradation of dye wastewaters. *Chemical Engineering and Processing: Process Intensification*, *71*, 59-69.

Gu, Z., Ma, Y., Yang, W., Zhang, G., Yao, J. (2005). Self-assembly of highly oriented one-dimensional h-WO_3 nanostructures. *Chem. Commun.*, *28*, 3597–3599.

Huang, Q., Wei, W., Sun, J., Mao, S., & Ni, B. (2019). Hexagonal K_2W_4O13 Nanowires for the Adsorption of Methylene Blue. *ACS Applied Nano Materials*, 2(6), 3802-3812.

Karaoğlu, M.H., Kula, İ. & Uğurlu, M. (2013). Adsorption Kinetic and Equilibrium Studies on Removal of Lead(II) onto Glutamic Acid/Sepiolite. *CLEAN Soil Air Water*, *41*(6), 548-556.

Kataria, N., & Garg, V. K. (2017). Removal of Congo red and Brilliant green dyes from aqueous solution using flower shaped ZnO nanoparticles. *Journal of Environmental Chemical Engineering*, *5*(6), 5420-5428.

Keiteb, A.S., Saion, E., Zakaria, A., & Soltani, N. (2016). Structural and optical properties of zirconia nanoparticles by thermal treatment synthesis. *Journal of Nanomaterials*, *2016*, 1913609. Retrieved from https://doi.org/10.1155/2016/1913609.

Khan, M. Y., Ahmad, M., Sadaf, S., Iqbal, S., Nawaz, F., & Iqbal, J. (2019). Visible light active indigo dye/graphene/WO_3 nanocomposites with excellent photocatalytic activity. *Journal of Materials Research and Technology*, *8*(3), 3261-3269.

Kyriakopoulos, G., & Doulia, D. (2006). Adsorption of pesticides on carbonaceous and polymeric materials from aqueous solutions: A review. *Separation and Purification Reviews*, 35 (3), 97-191.

Li, W., Cao, L., Kong, X., Huang, J., Yao, C., Fei, J., & Li, J. (2016). In situ synthesis and photocatalytic performance of WO_3/$ZnWO_4$ composite powders. *RSC Advances*, 6(28), 23783-23789.

Liu, G., Wang, S., Nie, Y., Sun, X., Zhang, Y., & Tang, Y. (2013). Electrostatic-induced synthesis of tungsten bronze nanostructures with excellent photo-to-thermal conversion behavior. *Journal of Materials Chemistry A*, *1*(35), 10120-10554. DOI: 10.1039/C3TA11479A

Naseem, Z. (2012). Lead Removal from Water by Low Cost Adsorbents: A Review. *Pak. J. Anal. Environ. Chem.*, *13*, 1-8.

Mayor, S. (2017). Pollution is linked to one in six deaths worldwide, study estimates. *BMJ*, j4884. DOI:10.1136/bmj.j4844

Nandi, B.K., Goswami, A., & Purkait, M.K. (2008). Adsorption characteristics of brilliant green dye on kaolin. *Journal of Hazardous Materials*, 161, 1, 387-395.

Ogugbue, C.J., Sawidis, T. (2011). Bioremediation and Detoxification of Synthetic Wastewater Containing Triarylmethane Dyes by Aeromonas hydrophila Isolated from Industrial Effluent. *Biotechnology Research International*, *2011*, 967925.

Ogunlalu, O.U., Aderibigbe, A.D., Oluwasina, O.O., & Amoo, I.A. (2017). Adsorption studies of Pb^{2+} from aqueous solutions using unmodified and citric acid - modified Plantain (Musa paradisiaca) Peels. *IOSR Journal of Applied Chemistry*, *10*(2), 30-39.

Shah, A. T., Din, M. I., Kanwal, F. N., & Mirza, M. L. (2015). Direct synthesis of mesoporous molecular sieves of Ni-SBA-16 by internal pH adjustment method and its performance for adsorption of toxic Brilliant Green dye. *Arabian Journal of Chemistry*, *8*(4), 579-586.

Silva, C. R., Gomes, T. F., Andrade, G. C., Monteiro, S. H., Dias, A. C., Zagatto, E. A., & Tornisielo, V. L. (2013). Banana Peel as an Adsorbent for Removing Atrazine and Ametryne from Waters. *J. Agric. Food Chem, 61*, 2358-2363.

Sönmezaym, A., Öncel, M. S.,& Bektaş, N. (2012). Adsorption of lead and cadmium ions from aqueous solutions using manganoxide minerals. *Transactions of Nonferrous Metals Society of China*, *22*(12), 3131-3139.

Supothina, S., Suwan, M., & Wisitsoraat, A. (2014) Hydrothermal synthesis of $K_2W_4O_{13}$ nanowire with high H_2S gas sensitivity. *Microelectronic Engineering*, *126*, 88-92.

Valica, M., & Hostin, S. (2016). Electrochemical treatment of water contaminated with methyl orange. *Nova Biotechnologica et Chimica*, *15*(1), 55-64.

Wang, F., Zhang, H., Chen, Z., Zhang, M., & Zhang, L. (2011). Kinetics and Possible Mechanism of the Degradation of Methyl Orange by Microwave Assisted with Fenton Reagent. *2011 5th International Conference on Bioinformatics and Biomedical Engineering*, Wuhan: Institute of Electrical and Electronics Engineer, 1-4.

Wani, A. L., Ara, A., & Usmani, J. A. (2015). Lead toxicity: A review. *Interdisciplinary Toxicology*, 8(2), 55-64.

Wu, X., Wang, J., Zhang, G., Katsumata, K., Yanagisawa, K., Sato, T., Yin, S. (2017). Series of M_xWO_3/ZnO (M =K, Rb, NH_4) nanocomposites: Combination of energy saving and environmental decontamination functions. *Applied Catalysis B: Environmental*, *201*, 128–136.

Yardley, J. (2013). Bangladesh Pollution Told in Colours and Smells. *The New York Times*. Retrieved from https://www.nytimes.com/2013/07/15/world/asia/bangladesh-pollution-told-in-colors-and-smells.html

Yu, X., Hou, T., Li, Y., Sun, X., & Lee, S.T. (2013). Effective band gap reduction of titanium oxide semiconductors by codoping from first-principles calculations. *International journal of quantum chemistry*, *113*(23), 2546-2553.

Zhao, Z., Ping, N., Di, J., & Zheng, H. (2016). Highly selective adsorption of organic dyes onto tungsten trioxide nanowires. *Research on Chemical Intermediates*, *42*, 5639-5651.

Zhou, Z., Kong, B., & Yu, C. (2014) Tungsten oxide nanorods: an efficient nanoplatform for tumor CT imaging and photothermal therapy. *Scientific Reports*, *4*, 3653. DOI: 10.1038/srep03653

Appendix - Equilibrium adsorption isotherm studies on $K_2W_4O_{13}$ nanowires

Adsorption of brilliant green dye

The equilibrium concentration data of adsorption of brilliant green and lead(II) ions was fitted into the Langmuir and Freundlich linearized isotherm models as given in Equation 7 and Equation 8, respectively:

$$\frac{C_e}{Q_e} = \frac{1}{bQ_m} + \frac{C_e}{Q_{max}} \quad (7)$$

$$\log(Q_e) = \log(K_F) + \frac{1}{n}\log(C_e) \quad (8)$$

Where C_e refers to the equilibrium concentration of the pollutant (mg/L), Q_e is the adsorption capacity (mg/g), Q_{max} is the maximum adsorption capacity (mg/g), b is the Langmuir constant which indicates the sorption intensity. K_F is a constant related to sorption capacity and n corresponds to sorption intensity.

The Langmuir model assumes that adsorbed material (such as lead(II) ions) is adsorbed over a homogenous adsorbent surface at a constant temperature. The Freundlich model, however, assumes that adsorption occurs over a heterogenous surface. If the equilibrium concentration data fits the Langmuir isotherm model, adsorption can be inferred to be monolayer. Important information such as the maximum adsorption capacity can be derived from the inverse of the gradient of the Langmuir linear equation. In contrast, if the equilibrium concentration data fits the Freundlich isotherm, adsorption can be inferred to occur on a heterogenous surface and adsorption is multilayer.

Figure 10 shows the linearized Langmuir plot, where its gradient was used to calculate the maximum adsorption capacity (Q_{max}), which are tabulated in Table 3. Figure 11 shows the linearized Freundlich plot. The correlation coefficients (R^2) indicate that the Langmuir model fits the adsorption data better. Maximum adsorption capacity on brilliant green dye was determined to be 476 mg g^{-1}.

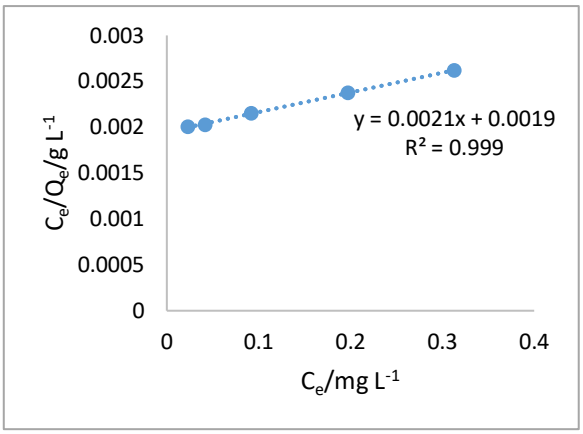

Figure 10: Langmuir isotherm for brilliant green dye

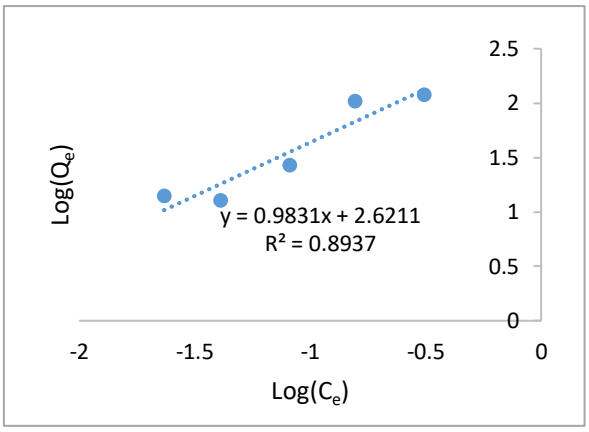

Figure 11: Freundlich isotherm for brilliant green dye

Table 3: The isotherm parameters for the adsorption of brilliant green dye by $K_2W_4O_{13}$ nanowires

Pollutant	**Langmuir**			**Freundlich**
	Q_m (mg g^{-1})	**b (L mg^{-1})**	**R^2**	**R^2**
Brilliant green dye	476	1.11	0.999	0.8937

Adsorption of lead(II) ions

Figure 12 shows the linearized Langmuir plot for lead(II) ions, where its gradient was used to calculate the Q_m (maximum adsorption capacity), which are tabulated in Table 4. Figure 13 shows the linearized Freundlich plot. The correlation coefficients (R^2) indicate that the Langmuir model again fits the adsorption data better.

Maximum adsorption capacity on lead(II) ions was determined to be 175 mg g^{-1}.

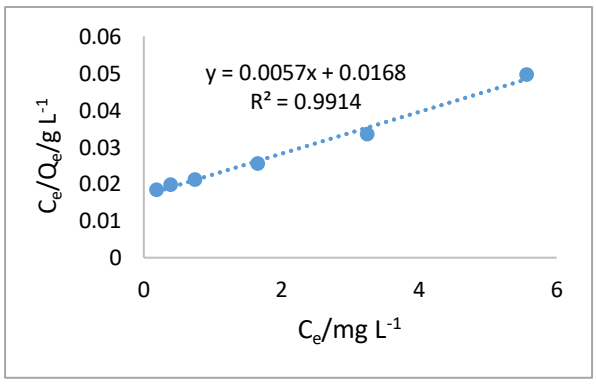

Figure 12: Langmuir isotherm for lead(II) ions

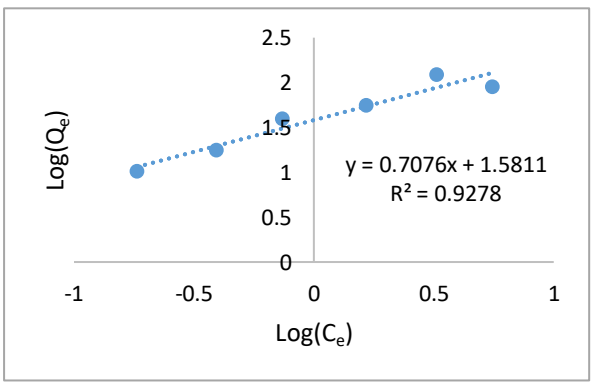

Figure 13: Freundlich isotherm for lead(II) ions

Table 4: Isotherm parameters for the adsorption of Pb^{2+} ions by $K_2W_4O_{13}$ nanowires

Pollutant	**Langmuir**			**Freundlich**
	Q_m (mg g^{-1})	**b (L mg^{-1})**	**R^2**	**R^2**
Lead(II) ions	175	0.339	0.9914	0.9287

Structure of $K_2W_4O_{13}$ nanowires

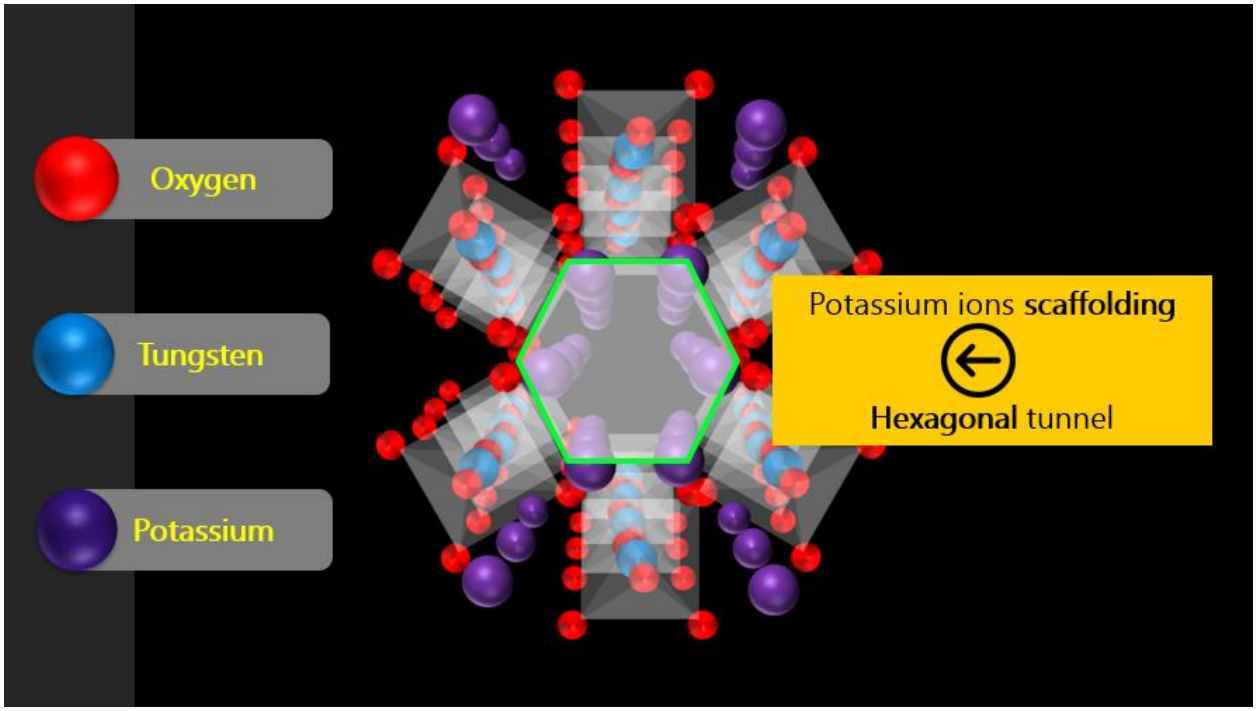

Figure 14: Structure of $K_2W_4O_{13}$ nanowires

$K_2W_4O_{13}$ nanowires are formed by WO_6 octahedra which share the axial oxygen atoms to form a hexagonal tunnel. Potassium ions are intercalated into the crystal lattice of the hexagonal WO_6 atoms, hence forming the $K_2W_4O_{13}$ nanowires.